Relativistic many-body calculation of energies, multipole transition rates, and lifetimes in tungsten ions

U. I. Safronova, M. S. Safronova, and N. Nakamura

Phys. Rev. A **95**, 042510 — Published 18 April 2017

DOI: 10.1103/PhysRevA.95.042510

Relativistic many-body calculation of energies, multipole transition rates, and lifetimes in tungsten ions

U. I. Safronova
Physics Department, University of Nevada, Reno, Nevada 89557

M. S. Safronova
Department of Physics and Astronomy, 217 Sharp Lab, University of Delaware, Newark, Delaware 19716 and Joint Quantum Institute, NIST and the University of Maryland, College Park, Maryland, USA

N. Nakamura
Institute for Laser Science, The University of Electro-Communications, Tokyo 182-8585, Japan

Atomic properties of Cd-like W^{26+}, In-like W^{25+}, and Sn-like W^{24+} ions are evaluated using a relativistic CI+all-order approach that combines configuration interaction and the coupled-cluster methods. The energies, transition rates, and lifetimes of low-lying levels are calculated and compared with available theoretical and experimental values. The magnetic-dipole transition rates are calculated to determine the branching ratios and lifetimes for the $4f^3$ states in W^{25+} and for the $4f^4$ in W^{24+} ions. Excellent agreement of the CI+all-order values provided a benchmark test of this method for the $4f^n$ configurations validating the recommended values of tungsten ion properties calculated in this work.

I. INTRODUCTION

The spectra of tungsten ions are important for plasma diagnostics. Tungsten has been selected as a plasma-facing material in International Thermonuclear Experimental Reactor (ITER), which is an experimental fusion reactor under construction. Thus, tungsten ions are considered to be the main impurity in the ITER plasma [1]. In order to suppress the radiation loss due to the emission of the impurity tungsten ions, it is important to understand the influx and the charge evolution of tungsten ions in the plasma through spectroscopic diagnostics. However, spectroscopic data of tungsten required for the diagnostics are by far insufficient because the required data span wide ranges of charge states and wavelengths [2, 3]. In particular, transitions in the visible range are strongly demanded due to the advantage that a variety of common optical components, such as mirrors, lenses, and fiber optics, can be applied. Thus, recently experimental and theoretical efforts have been maid to accumulate the spectroscopic data of tungsten ions in the visible range. However, spectra identifications presented a very difficult task due to a large number of transitions and paucity of precision theoretical data. In this work, we carry out a systematic study of tungsten ions to provide much needed theoretical benchmarks. We select ions with several $4f$ valence electrons, which present a particular difficult theoretical problem due to large core-valence correlations. This is the first treatment of these ions with a high-precision approach that takes into account these corrections to all-order paving the way to high-precision treatment of $4f^n$ configurations for a variety of systems and applications.

There is also much interest in the spectra of highly charged ions (HCI) with a few nf valence electrons due to a completely different application to the development of the high-precision optical frequency standards with HCIs and searches for the variation of fundamental constants [4] and the violation of Lorentz invariance [5]. Recent studies of uncertainties [6–8] have shown that the fractional accuracy of the transition frequency in the clocks based on HCI can be smaller than 10^{-19} since highly charged ions are less sensitive to external perturbations than either neutral atoms or singly charged ions due to their more compact size. In 2015, a crucial step have been achieved toward practical realization of HCI clocks with a breakthrough demonstration of sympathetic cooling of Ar^{13+} with laser-cooled Be^+ Coulomb crystal in cryogenic 4K Paul trap [9]. A major roadblock toward further progress in this fields is the lack of experimental measurements and accurate theoretical description for most of the potential clock candidates. The proposed HCIs generally have one or more nf valence electrons and benchmark tests of theory accuracy for such configurations provide additional motivation for this work besides the plasma physics applications.

We start with an overview of the current status of tungsten ion studies relevant to the present work. An investigation of the M1 transitions of the ground-state configuration of In-like tungsten was recently presented by Li *et al.* [10]. Three visible lines of M1 transitions from In-like tungsten were recorded using the Shanghai Permanent Magnet Electron Beam Ion Trap (EBIT). The experimental vacuum wavelengths were measured as 493.84± 0.15 nm, 226.97± 0.13 nm and 587.63 ±0.23 nm. These results are in good agreement with theoretical predictions obtained using the large-scale relativistic many-body perturbation theory. Cascade emission in electron beam ion trap plasma of W^{25+} ion was investigated by Jonauskas *et al.* [11]. Spectra of the W^{25+} ion were studied using

the collisional-radiative model (CRM) with an ensuing cascade emission. This work established that the cascade emission was responsible for the disappearance of the line structure at about 6 nm in the EBIT plasma. Emission band at 4.5-5.3 nm was also affected by the cascade emission. The strongest lines in the CRM spectrum correspond to $4d^9 4f^4 \to 4f^3$ transitions, while $4f^2 5d \to 4f^3$ transitions arise after the cascade emission is taken into account [11].

The large-scale relativistic configuration interaction calculations of W^{25+} spectroscopic properties [12] determined dominant contributions to the $4f^3$, $4d^9 4f^4$, $4f^2 5s$, $4f^2 5p$, $4f^2 5d$, $4f^2 5f$, $4f^2 5g$, and $4f^2 6g$ configurations. This study demonstrated that the correlation effects were crucial for the calculation of the $4f^2 5s \to 4f^3$ transition rate. In a single-configuration approach, this is an extremely weak electric-octupole transitions. Inclusion of the correlation effects increases the $4f^2 5d \to 4f^3$ transition probabilities by an order of magnitude. The corona model has been used to estimate the contribution of various transitions to the emission in a low-density EBIT plasma. Modeling in the 10-30 nm wavelength range produced lines which do not form emission bands and can be observed in the EBIT plasma [11].

The energy levels and radiative transition probabilities for the electric quadrupole and magnetic dipole transitions between the levels of the ground configuration, $[Kr]4d^{10}4f^4$, of W^{24+} were evaluated by Gaigalas *et al.* [13] using the large-scale multiconfiguration Hartree-Fock and Dirac-Fock calculations. The relativistic corrections were taken into account in the quasirelativistic Breit-Pauli and fully relativistic Breit approximations, also taking into account QED effects. The role of correlation, relativistic, and QED corrections was discussed. Line strengths, oscillator strengths, and transition probabilities in the Coulomb and Babushkin gauges were presented. Line strengths, oscillator strengths, and transition probabilities were presented for the E1 and E3 transitions in [14]. The large-scale nonrelativistic and relativistic calculations of the 977 lowest energy levels of W^{24+} was performed in [15]. The wavelengths of the electric dipole transitions, line strengths, transition probabilities, and the lifetimes of the lowest excited levels were calculated [15]. The accuracy of the LS- and jj-coupling schemes was discussed.

The two-electron tungsten ions were investigated in Refs. [16–19]. *Ab initio* multi-configuration Dirac-Fock calculation of M1 visible transitions among the ground state multiplets of the W^{26+} ion was performed in [16]. Theoretical investigation of spectroscopic properties of W^{26+} in EBIT plasma was recently presented by Jonauskas *et al.* [17]. Energy levels, radiative transition wavelengths and probabilities were studied for the W^{26+} ion using multiconfiguration Dirac-Fock and Dirac-Fock-Slater methods. Corona and collisional-radiative models have been applied to determine lines and corresponding configurations in a low-density EBIT plasma. Forbidden-line spectroscopy of the ground-state configuration of Cd-like W was used in [18] to identify several energy levels in cadmium-like tungsten, W^{26+}. The line identifications were supported by the large-scale multiconfiguration Dirac-Hartree-Fock and by relativistic many-body perturbation theory (RMBPT) calculations. The authors identified all seven lines and measured the corresponding wavelengths [18].

TABLE I: Energies (cm^{-1}) of the $4f^2$ excited states of Cd-like W^{26+} calculated using the CI+MBPT and CI+all-order methods are compared with other theoretical [16, 18] and experimental [18] values. All energies are given relative to the ground state.

Level	MBPT	All	Th. [16]	Th. [18]	Expt. [18]	Expt. [18]
$4f^2\ ^3H_4$	0	0	0	0	0	0
$4f^2\ ^3F_2$	18106	18024	18639	17819	18250	17891
$4f^2\ ^3H_5$	25896	25591	25747	25722	25678	25678
$4f^2\ ^1G_4$	38243	37999	38289	37854	37985	37985
$4f^2\ ^3F_3$	38407	37900	38555	37885	38184	37806
$4f^2\ ^3H_6$	47630	47125	47127	47215	47200	47200
$4f^2\ ^3F_4$	68621	67872	72843	67809	67948	67768
$4f^2\ ^1D_2$	69447	68992	70621	68249		
$4f^2\ ^3P_0$	71327	71137	67829	70440		
$4f^2\ ^3P_1$	83807	83448	85223	82955		
$4f^2\ ^1I_6$	87997	87740	89028	87010		
$4f^2\ ^3P_2$	103842	103114	104601	102616		
$4f^2\ ^1S_0$			177420	173588		

The spectra of W^{19+} - W^{32+} ions were observed in the EUV region between 15Å and 55Å in [20] using an EBIT and grazing-incidence spectrometer at the National Institute for Fusion Science. The electron energy dependence of the spectra was investigated for electron energies from 490 eV to 1320 eV. An identification of the observed lines was aided by collisional-radiative modeling of CoBIT plasma. The ion charge dependence of the $6g-4f$, $5g-4f$, $5f-4d$, $5p-4d$, and $4f-4d$ transition wavelengths were measured [20]. Komatsu *et al.* [21] reported the results for visible transitions in highly charged tungsten ions W^{q+} in the 365 - 475 nm region observed with a compact EBIT for the charge-state range of $q = 8-28$. More than a hundred previously-unreported lines were presented, and the charge state of the ions emitting the lines was identified from the electron energy dependence of the spectra.

In the present paper, we evaluate the atomic properties of Cd-like W^{26+}, In-like W^{25+}, and Sn-like W^{24+} ions using the CI+all-order approach which combines configuration interaction and the linearized coupled-cluster method with single and double excitations. The energies, transition rates, and lifetimes of low-lying levels are evaluated. Energies obtained using the CI+all-order code are compared with available theoretical and experimental values. We calculate magnetic-dipole and electric-quadrupole transition rates to determine the branching

TABLE II: Energies (cm^{-1}) of the $4f^3$ states of In-like W^{25+} calculated using the HULLAC code and the CI+all-order method are compared with other theoretical values [12]. All energies are given relative to the ground state.

Level	HULLAC	CI+all	GRASP2K[12]	Level	HULLAC	CI+all	GRASP2K[12]
$4f^3\ ^4I_{9/2}$	0	0	0	$4f^3\ ^4F_{3/2}$	38751	34599	35838
$4f^3\ ^4H^1_{9/2}$	46187	44672	44177	$4f^3\ ^4P_{3/2}$	56569	53184	54612
$4f^3\ ^4G^1_{9/2}$	72350	69938	69991	$4f^3\ ^4D^1_{3/2}$	83540	78435	80259
$4f^3\ ^4G^2_{9/2}$	86728	82279	83690	$4f^3\ ^4D^2_{3/2}$	101401	94662	96991
$4f^3\ ^2G^1_{9/2}$	105208	102166	102260	$4f^3\ ^4D^3_{3/2}$	118274	112065	114213
$4f^3\ ^4H^2_{9/2}$	124107	117882	120419	$4f^3\ ^2D_{3/2}$	136691	130901	132593
$4f^3\ ^2G^2_{9/2}$	171914	159191	164876				
$4f^3\ ^4I_{11/2}$	19406	20032	19809	$4f^3\ ^2F_{5/2}$	51775	48277	49166
$4f^3\ ^4H^1_{11/2}$	74377	72276	72222	$4f^3\ ^4G_{5/2}$	60915	55863	57750
$4f^3\ ^4H^2_{11/2}$	97547	92765	94345	$4f^3\ ^2D^1_{5/2}$	93982	87869	89992
$4f^3\ ^2H^1_{11/2}$	106986	101762	104658	$4f^3\ ^2D^2_{5/2}$	102997	97131	98446
$4f^3\ ^2H^2_{11/2}$	141589	134794	138149	$4f^3\ ^4F^1_{5/2}$	134640	126456	128683
				$4f^3\ ^4F^2_{5/2}$	158192	149868	152149
$4f^3\ ^2I^1_{13/2}$	36718	37028	36809				
$4f^3\ ^2K_{13/2}$	74329	72560	73753	$4f^3\ ^2F^1_{7/2}$	57679	54969	55013
$4f^3\ ^2I^2_{13/2}$	118488	113082	116673	$4f^3\ ^4G^1_{7/2}$	69526	65368	66752
				$4f^3\ ^4G^2_{7/2}$	83267	80852	80706
$4f^3\ ^2I_{15/2}$	52108	51696	51581	$4f^3\ ^4D_{7/2}$	122226	113748	116679
$4f^3\ ^2K^1_{15/2}$	88285	85020	87228	$4f^3\ ^2F^1_{7/2}$	158066	148673	151074
$4f^3\ ^4L_{15/2}$	118149	114341	117238	$4f^3\ ^2G_{7/2}$	175837	162935	168915

ratios and lifetimes for the $4f^2$ states in W^{26+}, for the $4f^3$ states in W^{25+}, and for the $4f^4$ states in W^{24+} ions. None of the previous calculations included benchmark tests of the energies of the $4f^3$ configuration. Four valence $4f$ electrons have not yet previously been considered with the CI+all-order method.

II. CI+ALL-ORDER METHOD

The main idea of the CI + all-order approach introduced in [22] is the construction of the effective Hamiltonian calculated using a modified version of the linearized coupled-cluster method with single and double excitations (LCCSD) described in [23, 24]. The effective Hamiltonian contains dominant core and core-valence correlation corrections to all orders, treated with the same accuracy as in the all-order approach for the monovalent systems, where the highest theoretical accuracy has been achieved. The CI method is then used to treat valence-valence correlations [22, 25–27].

The CI + all-order approach is based on the Brillouin-Wigner variant of the many-body perturbation theory, rather than the Rayleigh-Schrödinger variant. The use of the Rayleigh-Schrodinger MBPT for systems with more than one valence electron leads to a nonsymmetrical effective Hamiltonian and to the problem of the "intruder states". In the Brillouin-Wigner variant of MBPT, the effective Hamiltonian is symmetric and accidentally small denominators do not arise; however, the effective Hamiltonian becames energy dependent leading to the introduction of the $\tilde{\epsilon}_v$ parameter in the practical implementation of the method as described in [22]. When $\tilde{\epsilon}_v$ is taken to be equal to the Dirac-Fork energy of the corresponding orbital, the formulas coincide with the original implementation of the LCCSD method [28] based on the Rayleigh-Schrödinger MBPT, with the terms included in the CI subtracted out. We refer the reader to Ref. [22] for the formulas and detail description of the CI + all-order method. In this work, we follow the prescription of [22] and take $\tilde{\epsilon}_v$ to be the DF energy of the lowest valence state for each partial wave.

The CI+all-order method was used to evaluate properties of atomic systems with two to four valence electrons [29–36] and to calculate atomic properties of the superheavy elements No, Lr and Rf by Dzuba *et al.* [37, 38]. The $7s^2$ and $7snl$ states were considered for the nobelium atom, the $7s^26d$, and $7s7p6d$ states were considered for the lawrencium atom, and the $7s^26d^2$, $7s^27p6d$ and $7s7p6d^2$ states were considered for the rutherfordium atom [37]. The CI+all-order method was used to calculate energies in Ce, Ce^+, La, Ce^{2+}, and La^+, respectively [39] and to study various correlation corrections in these systems. The ground states in Ce^{2+} and La^+ are $4f^2\ ^3H_4$ and $5d^2\ ^3D_2$ rather than the $ns^2\ ^1S_0$.

TABLE III: Energies (cm^{-1}) of the $4f^4$ states of Sn-like W^{24+} calculated using the HULLAC code and the CI+all-order method are compared with other theoretical values [14]. All energies are given relative to the ground state.

Level	HULLAC	CI+all	MCDF[14]	Level	HULLAC	CI+all	MCDF[14]	Level	HULLAC	CI+all	MCDF[14]
$4f^4\ ^3P_0$	88785	82526	88190	$4f^4\ ^5I_4$	0	0	0	$4f^4\ ^5I_6^1$	25452	25823	25296
$4f^4\ ^5D_0$	94218	88424	92397	$4f^4\ ^3G_4^1$	46588	43458	43420	$4f^4\ ^3K_6$	57631	56846	55363
				$4f^4\ ^3F_4$	64400	61321	64874	$4f^4\ ^1G_6$	89983	85423	91126
$4f^4\ ^3D_1$	42684	39823	43817	$4f^4\ ^3G_4^2$	75778	71981	77687	$4f^4\ ^1H_6^1$	97318	93468	97237
$4f^4\ ^1P_1^1$	83001	80291	84017	$4f^4\ ^1F_4$	91009	86816	89877	$4f^4\ ^5I_6^2$	105151	101215	105066
$4f^4\ ^5D_1$	99407	91229	104330	$4f^4\ ^3G_4^3$	99883	95862	100434	$4f^4\ ^3I_6^1$	118814	113960	116199
$4f^4\ ^1P_1^2$	110318	107595	110949	$4f^4\ ^5G_4^1$	107647	100682	105784	$4f^4\ ^5K_6$	136283	127522	134183
				$4f^4\ ^5G_4^2$	118676	111437	119186	$4f^4\ ^5I_6^3$	140045	134127	139997
$4f^4\ ^5F_2^1$	39268	34776	35288	$4f^4\ ^1G_4$	126605	122041	124315	$4f^4\ ^5I_6^4$	156045	146934	156107
$4f^4\ ^3F_2^1$	54803	50423	56051	$4f^4\ ^3G_4$	134400	126816	134822	$4f^4\ ^1I_6$	169769	158159	169242
$4f^4\ ^5P_2$	55525	51659	57615	$4f^4\ ^5H_4$	139032	130491	139463	$4f^4\ ^3I_6^2$	192090	181250	192274
$4f^4\ ^3D_2$	76974	73898	76349	$4f^4\ ^5G_4^3$	143355	135393	144790	$4f^4\ ^1H_6^2$	233189	218508	233000
$4f^4\ ^5F_2^2$	85994	82792	86867								
$4f^4\ ^3F_2^2$	97991	92404	98747	$4f^4\ ^5I_5^1$	13294	13854	13423	$4f^4\ ^5I_7$	35910	35681	39480
$4f^4\ ^3P_2$	106620	99122	107889	$4f^4\ ^3G_5$	63109	59657	61769	$4f^4\ ^5L_7$	62243	60784	63218
$4f^4\ ^3S_2$	112648	109247	113696	$4f^4\ ^5G_5$	77444	74122	78338	$4f^4\ ^1K_7$	88340	87629	91087
$4f^4\ ^5F_2^3$	135320	130948	136278	$4f^4\ ^5H_5^1$	88110	84243	88343	$4f^4\ ^1I_7$	104815	100566	100459
$4f^4\ ^1D_2^1$	142342	133756	143622	$4f^4\ ^5I_5^2$	90797	86677	91504	$4f^4\ ^3K_7$	134403	129846	135090
$4f^4\ ^1D_2^2$	148027	143421	149290	$4f^4\ ^5H_5^2$	112600	108818	111372	$4f^4\ ^5K_7$	146509	137075	143837
				$4f^4\ ^3H_5^1$	123807	117093	124060				
$4f^4\ ^5F_3$	50166	46853	50586	$4f^4\ ^5H_5^3$	132002	126737	132341	$4f^4\ ^5I_8$	44954	44030	46638
$4f^4\ ^1F_3^1$	57899	53468	58388	$4f^4\ ^1H_5$	148107	138326	146263	$4f^4\ ^1L_8$	67884	65661	66920
$4f^4\ ^5G_3^1$	77622	74452	77823	$4f^4\ ^3H_5^2$	153058	146033	153431	$4f^4\ ^5M_8$	87598	85538	86878
$4f^4\ ^1D_3$	90352	86466	89636	$4f^4\ ^5I_5^3$	170059	159887	170505	$4f^4\ ^5L_8$	92979	91472	95051
$4f^4\ ^3D_3$	110168	105081	110895	$4f^4\ ^1G_5$	181102	167622	181127	$4f^4\ ^3L_8$	124642	123526	127190
$4f^4\ ^3F_3^1$	115494	108945	118936					$4f^4\ ^1K_8$	144505	135093	143232
$4f^4\ ^3F_3^2$	119258	113636	119986								
$4f^4\ ^5G_3^2$	134297	125837	136125								
$4f^4\ ^1F_3^2$	152469	143699	153325								
$4f^4\ ^5G_3^3$	172381	159733	172898								
$4f^4\ ^1F_3^3$	183652	170137	184264								

III. EXCITATION ENERGIES IN CD-LIKE W^{26+}, IN-LIKE W^{25+}, AND SN-LIKE W^{24+} IONS

The CI + all-order approach was used to evaluated energies of the $4f^2$ states in Cd-like W^{26+}, $4f^3$ states in In-like W^{25+}, $4f^4$ states in Sn-like W^{24+}. These $4f^n$ states are the lowest-lying states which do not mix with the $4f^{n-1}5l$ states. There are 13 $4f^2$ states in W^{26+}, 41 $4f^3$ states in W^{25+}, and 107 $4f^4$ states in W^{24+} ions. Excitation energies of these ions are listed in Tables I, II, and III, respectively. We compare the results of our CI + all-order *ab initio* calculations with theoretical results performed in Refs. [12, 14, 16, 18].

A. Energies of Cd-like W^{26+}

To estimate the accuracy of the CI + all-order results listed in the collum "CI+all-order" of Table I, we carried out another calculation using a CI+MBPT method [40], in which the effective Hamiltonian was calculated using a second-order MBPT, rather than all-order coupled-cluster method. The difference of the CI+all-order and CI+MBPT results gives an approximate contribution from the higher-order Coulomb correlations and serves as an estimate of the uncertainty of the results, as discussed by Safronova *et al.* [26]. Comparing energies given in the "CI+MBPT" and "CI+all-order" columns of Table I, we find that the difference is about 1%. Experimental results for seven identified lines are listed in two last columns of Table I. Due to the close degeneracy of two levels, authors provided alternative energies for three of the levels

listed in Table I. Our CI+all-order values are in excellent agreement with the experiment.

We also calculated the energies using a commonly used Hebrew University Lawrence Livermore Atomic Code (HULLAC) [41]. This code is based on the relativistic version of the parametric potential method, including configuration mixing. HULLAC results differ by up to 10% with the CI+all-order values and experimet. This is expected owing to more complete inclusion of the correlation corrections in the CI+all-order method.

The differences between the CI+all-order results and theoretical values from [16], obtained using multiconfiguration Dirac-Fock (MCDF) method implemented by the GRASP2K [42] and RATIP [43] packages, are 1-7%. The results of more recent 2014 calculation [18] performed using the large-scale multiconfiguration Dirac-Hartree-Fock calculations which involved careful investigations of core-valence and core-core correlation effects are in excellent agreement with the CI+all-order results. Only for the $4f^2\ {}^3F_2$ level, the difference is larger than 1%.

B. Energies of In-like W^{25+}

In Table II, we compare the energies of the $4f^3$ excited states of In-like W^{25+} calculated using the CI+all-order method with the GRASP2K code results from Ref. [12]. Since HULLAC is commonly used for such calculation for the line identification purposes, we also include HULLAC results. In general, we find CI+all-order and GRASP2K results in rather good agreement, the differences are 2% - 3.5% for 16 states listed in Table II and 0.1% - 1.0% for seven levels. The HULLAC results differ substantially from both CI+all-order values for most levels; with 5% -10% difference for 18 states listed in Table II.

C. Energies of Sn-like W^{24+}

In Table III, we compare excitation energies for 76 levels of the $4f^4$ configuration in Sn-like W^{24+} ion obtained by the CI+all-order codes with theoretical results in Ref. [14] and the HULLAC results. The results of Ref. [14] were obtained with the multiconfiguration Hartree-Fock (MCHF) and multiconfiguration Dirac-Fock (MCDF) approaches taking into account relativistic and QED corrections. The relativistic corrections were taken into account in the quasirelativistic Breit-Pauli and fully relativistic Breit approximations. The QED corrections are very small for the $4f^4$ states, 0.02% - 0.1% according to Table I of Ref. [14]. Somewhat unexpectedly, we find that MCDF results of [14] are close to HULLAC values, with the 0.1% - 1.0% agreement for 42 level $4f^4$ states. We would expect MCDF to be in better agreement with the CI+all-order values since we demonstrated that energies obtained by the HULLAC code shows the 10% disagreement with the results obtained by the CI+all-order and GRASP2k codes for the $4f^2$ and $4f^3$ states. We show below that the CI+all-order wavelengths are in excellent agrement with experiment for the transitions between the $4f^4$ states.

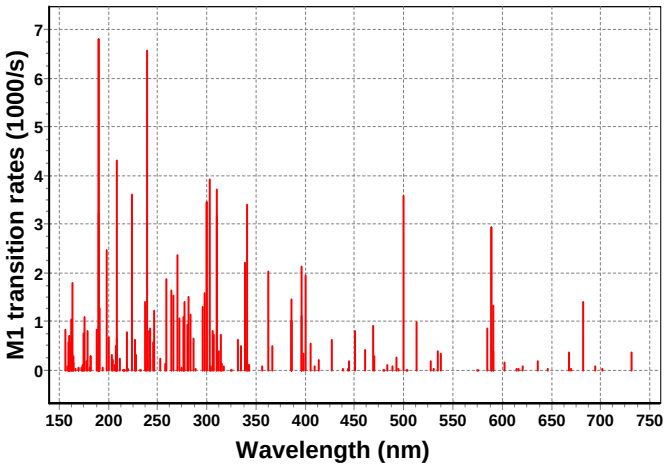

FIG. 1: Synthetic spectra of In-like W^{25+} ion based on the M1 transitions between the states of the $4f^3$ configuration. Results are obtained using CI+all-order code. The scale in the ordinate is in units of s^{-1}.

IV. MULTIPOLE MATRIX ELEMENTS AND TRANSITION RATES IN CD-LIKE W^{26+}

The multipole A_r^{Ek} (E1, E2, and E3) and A_r^{Mk} (M1, M2, and M3) transition probabilities in s^{-1} are obtained in terms of matrix elements Z_{Ek} and Z_{Mk} (a.u.), and transition energies ΔE (a.u.) as

$$A_r^{Ek} = \frac{C^{(k)}\,[\Delta E]^{2k+1}}{(2J+1)}\,(Z_{Ek})^2\,, \qquad (1)$$

$$C^{(1)} = 2.14200\times 10^{10},$$
$$C^{(2)} = 5.70322\times 10^{4},$$
$$C^{(3)} = 7.71311\times 10^{-2},$$

$$A_r^{Mk} = \frac{D^{(k)}\,[\Delta E]^{2k+1}}{(2J+1)}\,(Z_{Mk})^2\,, \qquad (2)$$

$$D^{(1)} = 2.85161\times 10^{5},$$
$$D^{(2)} = 7.59260\times 10^{-1},$$
$$D^{(3)} = 1.02683\times 10^{-6}.$$

In Table IV, we list CI+all-order wavelengths, multipole matrix elements $Z_{\rm M1}$, $Z_{\rm E2}$, and $Z_{\rm M3}$ and weighted $gA_r^{\rm M1}$ transition rates evaluated using the CI+all-order approach for 21 transitions between even-parity $4f^2$ levels of Cd-like W^{26+}. The random phase approximation (RPA) corrections to the multipole operators are included. The code packages for the calculation of matrix elements and the RPA corrections are the same for

TABLE IV: The wavelengths λ (in nm), absolute values of reduced matrix elements, and weighted radiative transition rates (in s^{-1}) of the $4f^2$ excited states of Cd-like W^{26+} ion calculated using the CI+all-order method. The E2 matrix elements are given in atomic units, the M1 and M3 matrix elements are in units of μ_B. The numbers in brackets represent powers of 10.

Transitions		λ	Matrix elements			s^{-1}
Lower	Upper		Z_{M1}	Z_{E2}	Z_{M3}	gA_r^{M1}
$4f^2\ ^3H_5$	$4f^2\ ^1G_4$	805.9	1.0125	0.0242	1.5836	5.28[01]
$4f^2\ ^1D_2$	$4f^2\ ^3P_1$	691.8	0.9161	0.1663	0.8957	6.84[01]
$4f^2\ ^3P_1$	$4f^2\ ^3P_2$	508.5	1.2700	0.1368	0.3763	3.31[02]
$4f^2\ ^3F_2$	$4f^2\ ^3F_3$	503.1	2.3815	0.0273	0.3090	1.20[03]
$4f^2\ ^3H_5$	$4f^2\ ^3H_6$	464.4	3.1605	0.0876	0.8989	2.69[03]
$4f^2\ ^3H_4$	$4f^2\ ^3H_5$	390.8	3.0617	0.0932	0.3286	4.24[03]
$4f^2\ ^1G_3$	$4f^2\ ^3F_4$	334.8	1.7725	0.0867	0.0840	2.26[03]
$4f^2\ ^3F_3$	$4f^2\ ^3F_4$	333.6	1.9022	0.0204	0.2580	2.63[03]
$4f^2\ ^1G_4$	$4f^2\ ^1D_2$	321.6	0.8772	0.1038	1.2044	6.24[02]
$4f^2\ ^1D_2$	$4f^2\ ^3P_2$	293.1	1.3722	0.0079	0.1954	2.02[03]
$4f^2\ ^3H_4$	$4f^2\ ^3F_3$	263.9	0.2503	0.0661	0.0584	9.20[01]
$4f^2\ ^3H_4$	$4f^2\ ^1G_4$	263.2	0.9898	0.0746	0.2723	1.45[03]
$4f^2\ ^3H_6$	$4f^2\ ^1I_6$	246.2	0.9632	0.0776	1.2535	1.68[03]
$4f^2\ ^3H_5$	$4f^2\ ^3F_4$	236.5	0.5140	0.0695	0.2911	5.39[02]
$4f^2\ ^3F_2$	$4f^2\ ^1D_2$	196.2	0.7103	0.0649	0.0141	1.80[03]
$4f^2\ ^3H_5$	$4f^2\ ^1I_6$	160.9	0.8400	0.0263	1.1908	4.57[03]
$4f^2\ ^1G_4$	$4f^2\ ^3P_2$	153.3	0.3776	0.1163	0.3603	1.07[03]
$4f^2\ ^3F_2$	$4f^2\ ^3P_1$	152.9	0.1345	0.1235	0.1644	1.37[02]
$4f^2\ ^3H_4$	$4f^2\ ^3F_4$	147.3	0.1549	0.0061	0.1270	2.02[02]
$4f^2\ ^3F_2$	$4f^2\ ^3P_2$	117.5	0.0594	0.0281	0.0699	5.85[01]

the CI+MBPT and CI+all-order approaches and are described in detail in Ref. [40]. The M1 transitions dominate for all levels. The ratios of the E2 and M1 transition rates are 10^{-3} - 10^{-7} for all transitions in Table IV with the exception of $^3F_2 - ^3P_1$. The E2/M1 ratio for this transition is 1.5×10^{-2}. The M3 transition rates are negligible for all levels, as expected, with the ratios of the M3 to M1 transition rates being 10^{-13} - 10^{-17}.

Wavelengths and weighted radiative transition rates for transitions between the $4f^2$ states in Cd-like W^{26+} are compared with theoretical and experimental results from Refs. [16, 18] in Table V. The theoretical results in Ref. [18] were obtained by different but complementary computational techniques, the multiconfiguration Dirac-Hartree-Fock (MCDHF) method implemented by the GRASP2K program suite and the multireference relativistic many-body perturbation theory (MR-RMBPT) calculations performed with the FAC code [44]. The identifications of the seven Cd-like lines observed in Ref. [18] were supported by large-scale multiconfiguration Dirac-Hartree-Fock calculations which involved careful investigations of core-valence and core-core correlation effects, and by relativistic many-body perturbation theory calculations. The Hg lamp as well as the Fe hollow cathode lamp were used for calibration [18]. We find an excellent agreement between our CI+all-order results and measurements from [18], the differences in wavelengths are 0.02% - 0.04% for the $^1G_4 - ^3F_4$, $^3F_3 - ^3F_4$, and $^3H_5 - ^3H_6$ transitions and the 0.2% - 0.4% for the $^1D_2 - ^3P_2$, $^1G_4 - ^3F_4$, $^3H_4 - ^3H_5$, and $^3F_2 - ^3F_3$ transitions. As in the case of the energy comparisons discussed above, the CI+MBPT wavelength results agree well with the 2014 theoretical results evaluated by GRASP2K code

TABLE V: Wavelengths (in nm) and weighted radiative transition rates (in s^{-1}) of the $4f^2$ excited states in Cd-like W^{26+} calculated using the CI+all-order code are compared with the results from Refs. [16, 18]. Note that the air wavelengths in [16] are corrected to the vacuum wavelengths. The numbers in brackets represent powers of 10.

Transition		λ	gA_r^{M1}	gA_r^{E2}
$4f^2\ ^1G_4 - 4f^2\ ^3F_4$	CI+all	263.2	1.45[3]	4.94[-2]
	Expt. [18]	263.261(12)		
	Th. [18]	262.1		
$4f^2\ ^3H_5 - 4f^2\ ^3H_6$	CI+all	464.4	2.69[3]	3.98[-3]
	Expt. [18]	464.64(15)		
	Expt. [16]	464.81(6)		
	Th. [18]	464.7		
	Th. [16]	467.79	2.66[3]	4.30[-3]
$4f^2\ ^1D_2 - 4f^2\ ^3P_2$	CI+all	293.1	2.02[3]	3.26[-4]
	Expt. [18]	291.890(11)		
	Th. [18]	293.5		
$4f^2\ ^3F_3 - 4f^2\ ^3F_4$	CI+all	333.6	2.63[3]	1.13[-3]
	Expt. [18]	333.748(9)		
	Th. [18]	334.4		
$4f^2\ ^3F_2 - 4f^2\ ^3F_3$	CI+all	503.1	1.20[03]	2.59[-04]
	Expt. [18]	502.15(17)		
	Expt. [16]	502.13(6)		
	Th. [18]	505.6		
	Th. [16]	501.80	1.22[3]	5.10[-4]
$4f^2\ ^1G_4 - 4f^2\ ^3F_4$	CI+all	334.8	2.26[3]	2.00[-2]
	Expt. [18]	335.758(11)		
	Th. [18]	334.5		
$4f^2\ ^3P_1 - 4f^2\ ^3P_2$	CI+all	508.5	3.31[2]	6.17[-3]
	Th. [16]	516.01	1.93[2]	
$4f^2\ ^1D_2 - 4f^2\ ^3P_1$	CI+all	691.8	6.84[1]	1.96[-3]
	Th. [16]	685.16	1.16[2]	4.79[-5]
$4f^2\ ^3H_4 - 4f^2\ ^3H_5$	CI+all	390.8	4.24[3]	1.07[-2]
	Expt. [18]	389.433(12)		
	Expt. [16]	389.52(6)		
	Th. [18]	390.9		
	Th. [16]	388.43	4.33[3]	1.86[-2]

TABLE VI: Wavelengths (in nm) in In-like W^{25+} calculated using the CI+all-order method are compared with measurements from Refs. [10, 21]. Note that the air wavelengths in [21] are corrected to the vacuum wavelengths. The M1 weighted radiative transition rates are given in the last column in s^{-1}. The numbers in brackets represent powers of 10.

Transitions		Expt.	Wavelengths, nm		Trans.
Lower	Upper	WL, nm	CI+all	HULLAC	CI+all
$^2F_{5/2}$	$^4D^2_{3/2}$		215.6	201.5	1.74[0]
$^4H^1_{11/2}$	$^4H^2_{9/2}$		219.3	201.1	7.86[2]
$^4D_{7/2}$	$^2G^2_{9/2}$		220.1	210.4	2.73[1]
$^4I_{9/2}$	$^4H^1_{9/2}$	226.97(13)[10]	223.9	209.2	3.60[3]
$^4P_{3/2}$	$^2D^2_{5/2}$		227.5	215.4	6.30[2]
$^4H^1_{9/2}$	$^4H^1_{11/2}$		362.3	354.7	2.01[3]
$^2F^1_{7/2}$	$^4G^2_{9/2}$		366.2	344.2	4.97[2]
$^2D^1_{5/2}$	$^4D_{7/2}$		386.4	354.0	1.44[3]
		384.10(6)[21]			
$^2F_{7/2}$	$^4G^2_{7/2}$		386.4	390.8	1.00[3]
		387.4[21]			
$^4H^1_{9/2}$	$^4G^1_{9/2}$		395.8	382.2	2.12[3]
$^4P_{3/2}$	$^4D^1_{3/2}$		396.0	370.8	1.12[3]
$^4H^2_{11/2}$	$^4H^2_{9/2}$		398.1	329.8	3.24[2]
$^4G_{5/2}$	$^4G^2_{7/2}$		400.2	426.9	1.94[3]
		400.99(6)[21]			
$^4I_{11/2}$	$^4H^1_{9/2}$		405.8	373.4	5.38[2]
		407.03(6)[21]			
$^2H^2_{11/2}$	$^2G^2_{9/2}$		409.9	376.5	6.54[1]
$^2D^1_{5/2}$	$^4D^3_{3/2}$		413.3	411.7	2.03[2]
		421.40(6)[21]			
$^4F^1_{5/2}$	$^4F^2_{5/2}$		427.1	424.6	6.14[2]
$^4G^1_{9/2}$	$^4H^2_{11/2}$		438.1	396.9	1.50[1]
$^4G^1_{7/2}$	$^2D^1_{5/2}$		444.4	408.9	1.81[2]
$^4F^1_{5/2}$	$^2F^1_{7/2}$		450.1	447.4	7.93[2]
		451.28(6)[21]			
$^2I^2_{13/2}$	$^2H^2_{11/2}$		460.6	432.9	4.01[2]
		467.72(6)[21]			
$^4G^2_{7/2}$	$^2G^1_{9/2}$		469.2	455.8	9.16[2]
		469.34(6)[21]			
$^4F_{3/2}$	$^4G_{5/2}$		470.3	451.2	2.88[2]
$^4H^1_{11/2}$	$^4H^2_{11/2}$		488.1	431.6	7.48[1]
$^4H^2_{11/2}$	$^2I^2_{13/2}$		492.2	477.5	2.56[2]
$^2K_{13/2}$	$^4H^2_{11/2}$		494.9	430.7	3.21[1]
$^4I_{9/2}$	$^4I_{11/2}$	493.84(15)[10] 493.76(6)[21]	499.2	3.58[3]	
$^2D_{3/2}$	$^4F^2_{5/2}$		527.2	465.1	1.78[2]
$^4D^3_{3/2}$	$^2D_{3/2}$		530.9	543.0	1.17[1]
$^2F_{5/2}$	$^4G^1_{7/2}$		585.1	520.0	8.58[2]
$^4I_{11/2}$	$^2I^1_{13/2}$	587.63(23)[10]	588.4	577.6	2.92[3]
$^4G^1_{7/2}$	$^4G^2_{9/2}$		591.3	581.3	1.31[3]
$^2D^2_{5/2}$	$^4D_{7/2}$		601.8	563.3	1.46[2]

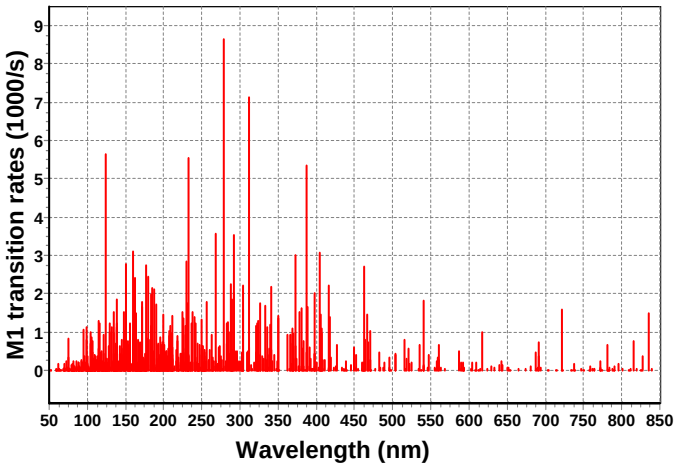

FIG. 2: Synthetic spectra of Sn like W^{24+} ion based on M1 transitions between the $4f^4$ states. Results are obtained busing CI-all-order code. The scale in the ordinate is in units of s^{-1}.

[18], from the 0.03% for the $^3H_4 - ^3H_5$ transition to the 0.50% for the $^3F_2 - ^3F_3$ transition. The differences with the 2011 MCDF results obtained also with GRASP2K [42] and RATIP [43] packages [16] are larger, 0.3 - 1%.

We also compare M1 and E2 transition rates with the avaliable values from the 2011 calculation [16]. We find good agreement for the M1 transition rates (1%-2%) for the $^3H_4 - ^3H_5$, $^3H_5 - ^3H_6$ and $^3F_2 - ^3F_3$ transitions, but very large differences for the $^3P_1 - ^3P_2$ and $^1D_2 - ^3P_1$ transitions. Large discrepancies are also found for the E2 transition rates but the contributions of the E2 transition rates are very small and should not be not important for spectra distributions of the W^{26+} - W^{24+} ions.

V. M1 TRANSITION RATES AND LIFETIMES IN IN-LIKE W^{25+}

The CI+all-order results for In-like W^{25+} are presented in Fig. 1 and Table VI. While we evaluated M1 and E2 matrix elements, the E2 contributions to the transition rates are negligible and are omitted.

We evaluated all possible M1 transitions between the levels listed in Table II. A complete set of of the $4f^3$ M1 transitions includes 360 transitions distributed in the 38 nm - 35211 nm region. In Fig. 1, we include the 157 transitions in the 150 nm - 750 nm wavelength region. Among these transitions, there are 44 transitions with M1 transition rate values larger than 1000 s^{-1}. The strongest M1 transitions are at 190 nm and 240 nm, with the weighted transition rates of 6800s^{-1} and 6570 s^{-1}, respectively.

The CI+all-order wavelengths are compared with measurements from Refs. [10, 21] in Table VI. In 2016, the wavelengths of three transitions in In-like W^{25+} were

TABLE VII: Energies (in cm^{-1}), wavelengths (in Å), magnetic-dipole transition rates, A_r (s^{-1}), branching ratios, and lifetimes τ (in ms) evaluated using the CI+all-order method in In-like W^{25+}. The numbers in brackets represent powers of 10.

Level	Transition		Energies		λ	Z^{M1}	A_r	Br. ratio	τ	τ [10]
$^4I_{11/2}$	$^4I_{9/2}$	$^4I_{11/2}$	0	20032	499.2	4.0618	2.98[2]	1.00	3.36	3.53
$^2I^1_{13/2}$	$^4I_{11/2}$	$^2I^1_{13/2}$	20032	37028	588.4	4.6945	2.09[2]	1.00	4.78	5.18
$^4H^1_{9/2}$	$^4I_{9/2}$	$^4H^1_{9/2}$	0	44672	223.9	1.2241	3.60[2]	0.87	2.42	2.68
	$^4I_{11/2}$	$^4H^1_{9/2}$	20032	44672	405.8	1.1547	5.38[1]	0.13		
$^2F_{5/2}$	$^4F_{3/2}$	$^2F_{5/2}$	34600	48278	731.1	2.3022	6.10[1]	1.00	16.39	18.05
$^2I_{15/2}$	$^2I^1_{13/2}$	$^2I_{15/2}$	37028	51696	681.8	4.0569	8.75[1]	1.00	11.43	12.71
$^4P_{3/2}$	$^4F_{3/2}$	$^4P_{3/2}$	34600	53184	538.1	1.3704	8.13[1]	0.99	12.18	12.23
$^2F^1_{7/2}$	$^4I_{9/2}$	$^2F^1_{7/2}$	0	54969	181.9	0.2550	3.64[1]	0.70	19.21	20.15
	$^4H^1_{9/2}$	$^2F^1_{7/2}$	44672	54969	971.2	1.7876	1.18[1]	0.23		
$^4G_{5/2}$	$^4F_{3/2}$	$^4G_{5/2}$	34600	55863	470.3	1.0531	4.80[1]	0.95	19.87	19.40
$^4G^1_{7/2}$	$^2F_{5/2}$	$^4G^1_{7/2}$	48278	65368	585.1	2.5244	1.07[2]	0.66	6.13	
	$^4I_{9/2}$	$^4G^1_{7/2}$	0	65368	153.0	0.1689	2.69[1]	0.17		
$^4G^1_{9/2}$	$^4H^1_{9/2}$	$^4G^1_{9/2}$	44672	69938	395.8	2.2098	2.12[2]	0.57	2.69	
	$^4I_{9/2}$	$^4G^1_{9/2}$	0	69938	143.0	0.2473	5.64[1]	0.15		
	$^4I_{11/2}$	$^4G^1_{9/2}$	20032	69938	200.4	0.4503	6.80[1]	0.18		
$^4H^1_{11/2}$	$^4H^1_{9/2}$	$^4H^1_{11/2}$	44672	72276	362.3	1.8813	1.68[2]	0.45	2.68	
	$^4I_{11/2}$	$^4H^1_{11/2}$	20032	72276	191.4	0.5763	1.07[2]	0.29		
	$^2I_{13/2}$	$^4H^1_{11/2}$	37028	72276	283.7	0.9860	9.58[1]	0.26		
$^2K_{13/2}$	$^4I_{11/2}$	$^2K_{13/2}$	20032	72560	190.4	1.3192	4.86[2]	0.82	1.68	
	$^2I^1_{13/2}$	$^2K_{13/2}$	37028	72560	281.4	1.1167	1.08[2]	0.18		
$^4D^1_{3/2}$	$^4P_{3/2}$	$^4D^1_{3/2}$	53184	78435	396.0	1.6090	2.80[2]	0.55	1.95	
	$^2F_{5/2}$	$^4D^1_{3/2}$	48278	78435	331.6	0.9091	1.53[2]	0.30		
	$^4F_{3/2}$	$^4D^1_{3/2}$	34600	78435	228.1	0.3601	7.38[1]	0.14		
	$^4F_{3/2}$	$^4D^1_{3/2}$	34600	78435	228.1	0.3601	7.38[1]	0.14		
$^4G^2_{7/2}$	$^2F_{7/2}$	$^4G^2_{7/2}$	54969	80852	386.4	1.4647	1.25[2]	0.27	2.15	
	$^4G_{5/2}$	$^4G^2_{7/2}$	55863	80852	400.2	2.1479	2.43[2]	0.52		
	$^2F_{5/2}$	$^4G^2_{7/2}$	48278	80852	307.0	0.8748	8.91[1]	0.19		
$^4G^2_{9/2}$	$^4H^1_{9/2}$	$^4G^2_{9/2}$	44672	82279	265.9	1.0277	1.52[2]	0.37	2.42	
	$^4G^1_{7/2}$	$^4G^2_{9/2}$	65368	82279	591.3	3.1724	1.31[2]	0.32		
	$^4I_{11/2}$	$^4G^2_{9/2}$	20032	82279	160.7	0.3282	7.01[1]	0.17		
	$^2F^1_{7/2}$	$^4G^2_{9/2}$	54969	82279	366.2	0.9511	4.97[1]	0.12		
$^2K_{15/2}$	$^2I^1_{13/2}$	$^2K_{15/2}$	37028	85020	208.4	1.2023	2.69[2]	0.54	2.00	
	$^2I_{15/2}$	$^2K_{15/2}$	51696	85020	300.1	1.8563	2.15[2]	0.43		
$^2D^1_{5/2}$	$^4F_{3/2}$	$^2D^1_{5/2}$	34600	87869	187.7	0.4524	1.39[2]	0.50	3.57	
	$^4G_{5/2}$	$^2D^1_{5/2}$	55863	87869	312.4	0.6599	6.42[1]	0.23		
	$^2F_{5/2}$	$^2D^1_{5/2}$	48278	87869	252.6	0.3768	3.97[1]	0.14		
	$^4G^1_{7/2}$	$^2D^1_{5/2}$	65368	87869	444.4	0.7670	3.02[1]	0.11		
$^4H^2_{11/2}$	$^2I^I_{13/2}$	$^4H^2_{11/2}$	37028	92765	179.4	0.4164	6.75[1]	0.39	5.80	
	$^4H^1_{9/2}$	$^4H^2_{11/2}$	44672	92765	207.9	0.4061	4.13[1]	0.24		
	$^4I_{11/2}$	$^4H^2_{11/2}$	20032	92765	137.5	0.1609	2.24[1]	0.13		
	$^4I_{9/2}$	$^4H^2_{11/2}$	0	92765	107.8	0.1008	1.83[1]	0.11		

TABLE VIII: Wavelengths (nm) and weighted radiative transition rates (in s^{-1}) of the $4f^4$ excited states in Sn-like W^{24+} calculated using the CI+all-order method are compared with theoretical results from Ref. [13]. HULLAC wavelengths are given for comparison. The numbers in brackets represent powers of 10.

Transitions		Wavelengths			Tr. rates	
Lower	Upper	CI+all	HULLAC	Ref. [13]	CI+all	Ref. [13]
$4f^4\ ^5I_8$	$4f^4\ ^1I_7$	176.9	167.1	165.3	2.74[3]	2.59[3]
$4f^4\ ^5I_8$	$4f^4\ ^3K_7$	116.5	111.8	110.7	2.94[1]	5.20[1]
$4f^4\ ^5I_8$	$4f^4\ ^5K_7$	107.5	98.5	97.6	4.45[2]	3.68[2]
$4f^4\ ^1L_8$	$4f^4\ ^1I_7$	286.5	270.8	267.3	6.35[1]	7.65[1]
$4f^4\ ^1L_8$	$4f^4\ ^3K_7$	155.8	150.3	148.7	1.21[3]	1.08[3]
$4f^4\ ^1L_8$	$4f^4\ ^5K_7$	140.0	127.2	126.0	3.25[1]	9.60[1]
$4f^4\ ^5M_8$	$4f^4\ ^1I_7$	665.4	580.8	572.7	1.18[1]	1.45[1]
$4f^4\ ^5M_8$	$4f^4\ ^3K_7$	225.7	213.7	211.3	5.60[2]	6.15[2]
$4f^4\ ^5M_8$	$4f^4\ ^5K_7$	194.0	169.7	168.4	3.11[2]	2.45[2]
$4f^4\ ^5L_8$	$4f^4\ ^1I_7$	1099.6	844.8	838.1	3.24[0]	4.77[0]
$4f^4\ ^5L_8$	$4f^4\ ^3K_7$	260.6	241.4	239.3	7.73[0]	1.50[1]
$4f^4\ ^5L_8$	$4f^4\ ^5K_7$	219.3	186.8	185.7	1.21[2]	1.19[2]
$4f^4\ ^3L_8$	$4f^4\ ^5K_7$	738.1	1024.5	1014.0	1.16[0]	2.32[0]
$4f^4\ ^5L_7$	$4f^4\ ^1L_8$	2050.0	1772.8	1941.0	2.18[1]	3.09[1]
$4f^4\ ^5L_7$	$4f^4\ ^5M_8$	404.0	394.4	398.4	3.05[3]	3.42[3]
$4f^4\ ^5L_7$	$4f^4\ ^5L_8$	325.9	325.4	326.5	1.75[3]	1.99[3]
$4f^4\ ^5L_7$	$4f^4\ ^3L_8$	159.4	160.3	159.9	9.48[2]	1.01[3]
$4f^4\ ^5L_7$	$4f^4\ ^1K_8$	134.6	121.6	122.2	9.66[2]	1.45[3]
$4f^4\ ^1K_7$	$4f^4\ ^5L_8$	2602.1	2155.7	2466.0	9.42[0]	1.26[1]
$4f^4\ ^1K_7$	$4f^4\ ^3L_8$	278.6	275.5	278.0	8.63[3]	9.70[3]
$4f^4\ ^1K_7$	$4f^4\ ^1K_8$	210.7	178.0	180.9	5.05[1]	7.69[0]
$4f^4\ ^1I_7$	$4f^4\ ^3L_8$	435.5	504.4	500.3	1.79[1]	1.05[1]
$4f^4\ ^1I_7$	$4f^4\ ^1K_8$	289.6	252.0	254.5	2.68[2]	3.48[2]
$4f^4\ ^3K_7$	$4f^4\ ^1K_8$	1905.9	990.0	1060.0	2.53[0]	8.47[0]

measured with the Shanghai permanent magnet EBIT, 587.63±0.23, 493.84±0.15, and 226.97±0.13 [10]. The authors identified the transitions as $^4I_{11/2} - {}^4I_{13/2}$, $^4I_{9/2} - {}^4I_{11/2}$, and $^4I_{9/2} - {}^2H_{9/2}$. respectively, based on the comparison with their calculation. In Ref. [21], the wavelengths of nine transitions in In-like W^{25+} obtained with a compact EBIT in Tokyo are given without identification. Among them, 493.62±0.06 nm (air) (493.76±0.06 nm in vacuum) is considered to be identical with the line observed in Shanghai at 493.84±0.15; thus, it is listed as $^4I_{9/2} - {}^4I_{11/2}$ in Table VI. Wavelengths of another eight transitions are also listed in the table, but without identification. The CI+all-order values are in excellent agreement with all of the identified experimental values, demonstrating predictive power of our approach for unmeasured quantities.

The CI + all-order results for the magnetic-dipole transitions in In-like W^{24+} are listed in Table VII. The M1 matrix elements, transition rates, branching ratios, and lifetimes for the eighteen $4f^3$ states are given. The labels of 18 levels are in the first column. Next two columns of Table VII list possible transitions that give dominant contributions to the lifetimes. The energies of the lower and upper states, listed in Table II, are given for convenience. The vacuum wavelengths λ given in the next column in Å are determined from these energies. The values of the M1 matrix elements, listed in Table VII, include RPA corrections to the M1 operator as described in [22]. The absolute values of the reduced M1 matrix elements are given in units of Bohr magneton.

The results for the 72 M1 A_r transition rates are calculated from the wavelengths and reduced matrix elements. Only 41 transitions which give significant contributions to the lifetimes are listed in Table VII, together with the corresponding branching ratios. The lifetimes are obtained as

$$\tau = \frac{1}{\Sigma A_r},$$

where the denominator is the sum of all possible transition rates contributing to the level lifetime. The lifetimes are given in milliseconds.

Excitation energies and lifetimes of the lowest eight energy levels of the $4f^3$ configuration in In-like W were evaluated in Ref. [10] using the RMBPT code. The lifetime values from [10] are listed in the last column of Table VII. The CI+all-order and RMBPT [10] lifetimes are in relatively good (10%) agreement.

VI. M1 TRANSITION RATES AND LIFETIMES IN SN-LIKE W^{24+}

The CI+all-order results for Sn-like W^{24+} ion are presented in Fig. 2 and Tables VIII and IX. We evaluated all possible M1 transitions between the levels listed in Table III. A complete set of the $4f^4$ M1 transitions includes 823 transitions in the 50 nm - 5526 nm wavelength region. In Fig. 2, we include the 760 transitions in the 50 nm - 750 nm wavelength region. Among these transitions, we found 96 transitions with M1 transition rates values gA_r^{M1} larger than 1000 s^{-1}. The strongest transitions are at 276.6 nm and 312.2 nm with the corresponding weighted transition rates of 8630 s^{-1} and 7110 s^{-1}.

The wavelengths and M1 weighted radiative transition rates of the $4f^4$ excited states in Sn-like W^{24+} calculated using the CI+all-order method are compared in Table VIII with theoretical results from Ref. [13] obtained using the large-scale multiconfiguration Hartree-Fock and Dirac-Fock calculations. HULLAC results are also given for illustration of the code performance. The difference between the CI+all-order wavelengths and Ref. [13] are 10 - 15% for most of the transitions. The MCHF/MCDF results of Table VIII are within 1% from

TABLE IX: Wavelengths (in nm) of the $4f^4$ excited states in Sn-like W^{25+} calculated using the CI+all-order method and HULLAC codes are compared with measurements from Ref. [21]. The experimental air wavelengths are corrected to the vacuum wavelengths. The CI+all-order M1 weighted radiative transition rates (in s^{-1}) are given in the last column. The numbers in brackets represent powers of 10.

Transitions		Wavelengths			gA_r	Transitions		Wavelengths			gA_r
Lower	Upper	Expt.[21]	CI+all	HULLAC	CI+all	Lower	Upper	Expt.[21]	CI+all	HULLAC	CI+all
$4f^4\ ^3G_4^1$	$4f^4\ ^3G_4^2$		350.6	342.6	1.42[3]	$4f^4\ ^5G_4^3$	$4f^4\ ^5I_5^3$		408.3	374.5	2.48[2]
$4f^4\ ^5F_3$	$4f^4\ ^5G_3^1$		362.3	364.2	9.13[2]			408.70(6)			
		364.68(6)						410.09(6)			
$4f^4\ ^1F_4$	$4f^4\ ^3F_3^2$		372.9	231.0	6.30[2]	$4f^4\ ^3I_6^1$	$4f^4\ ^1H_5$		410.4	341.4	2.58[2]
$4f^4\ ^3P_2$	$4f^4\ ^5G_3^2$		374.3	361.3	2.94[2]			412.3			
		374.45(6)				$4f^4\ ^5I_6^3$	$4f^4\ ^1I_6$		416.1	336.4	2.70[1]
		375.81(6)				$4f^4\ ^3F_2^1$	$4f^4\ ^5G_3^1$		416.2	438.2	2.21[3]
$4f^4\ ^5H_5^2$	$4f^4\ ^5G_4^3$		376.3	325.1	5.87[0]	$4f^4\ ^1G_4$	$4f^4\ ^3H_5^2$		416.8	378.0	5.17[1]
$4f^4\ ^5G_5$	$4f^4\ ^5G_4^1$		376.5	331.1	8.78[1]	$4f^4\ ^5G_4^2$	$4f^4\ ^5G_4^3$		417.4	405.2	1.38[3]
$4f^4\ ^5F_2^2$	$4f^4\ ^3S_2$		378.0	375.2	1.50[3]	$4f^4\ ^3G_4^2$	$4f^4\ ^3G_4^3$		418.7	414.9	3.19[2]
$4f^4\ ^3F_3^1$	$4f^4\ ^5G_4^3$		378.1	358.9	8.05[1]			419.47(6)			
$4f^4\ ^1F_3^2$	$4f^4\ ^1F_3^3$		378.2	320.7	1.93[1]	$4f^4\ ^1H_6^1$	$4f^4\ ^3H_5^1$		423.3	377.5	4.58[1]
		379.75(6)						425.29(6)			
$4f^4\ ^5G_3^1$	$4f^4\ ^5G_4^1$		381.2	333.1	1.60[3]	$4f^4\ ^3F_2^1$	$4f^4\ ^3D_2$		426.0	451.0	8.86[1]
$4f^4\ ^1D_2^1$	$4f^4\ ^5G_3^3$		384.9	332.9	7.72[0]	$4f^4\ ^1G_6$	$4f^4\ ^5H_5^2$		427.4	442.1	6.47[2]
		386.34(6)				$4f^4\ ^1D_3$	$4f^4\ ^3F_3^1$		444.9	397.7	1.19[2]
$4f^4\ ^3D_3$	$4f^4\ ^5F_2^3$		386.6	397.6	4.67[2]			447.49(6)			
$4f^4\ ^1L_8$	$4f^4\ ^5L_8$		387.4	398.5	5.35[3]	$4f^4\ ^5F_2^2$	$4f^4\ ^3D_3$		448.7	431.5	2.76[2]
$4f^4\ ^3G_5$	$4f^4\ ^1G_6$		388.1	372.1	1.65[3]	$4f^4\ ^5P_2$	$4f^4\ ^3D_2$		449.7	466.2	6.01[2]
$4f^4\ ^5I_6^3$	$4f^4\ ^5I_5^3$		388.2	333.2	1.05[2]	$4f^4\ ^3F_3^1$	$4f^4\ ^5H_4$		464.1	424.8	2.10[1]
		390.00(6)				$4f^4\ ^5G_3^1$	$4f^4\ ^3G_4^3$		467.1	449.2	1.45[3]
$4f^4\ ^5I_6^2$	$4f^4\ ^5H_5^3$		391.8	372.4	5.85[2]			467.93(6)			
$4f^4\ ^3F_4$	$4f^4\ ^1F_4$		392.2	375.8	2.86[2]	$4f^4\ ^5I_5^3$	$4f^4\ ^3I_6^2$		468.1	453.9	7.26[2]
		392.73(6)				$4f^4\ ^5G_4^1$	$4f^4\ ^1G_4$		468.2	527.5	1.24[2]
$4f^4\ ^3D_3$	$4f^4\ ^5H_4$		393.5	346.4	1.91[1]			468.35(6)			
$4f^4\ ^1F_4$	$4f^4\ ^5G_4^2$		406.2	361.4	1.43[3]	$4f^4\ ^3F_2^2$	$4f^4\ ^3F_3^2$		471.0	470.2	1.01[3]
		406.60(6)				$4f^4\ ^3G_4^3$	$4f^4\ ^3H_5^1$		471.0	418.0	2.42[2]
$4f^4\ ^3G_5$	$4f^4\ ^5H_5^1$		406.7	400.0	1.08[3]			471.31(6)			
$4f^4\ ^5H_5^1$	$4f^4\ ^5H_5^2$		406.9	408.3	9.67[2]	$4f^4\ ^1F_3^1$	$4f^4\ ^5G_3^1$		476.6	507.0	4.19[1]
$4f^4\ ^3S_2$	$4f^4\ ^1D_2^1$		408.0	336.8	1.31[1]						

the HULLAC data. Most likely, the MCHF/HULLAC differences with the CI+all-order values are due to accurate inclusion of the core-valence correlation effects in the CI+all-order method, but not either MCHF or HULLAC codes.

The M1 matrix elements, transition rates, branching ratios, and lifetimes for the eighteen $4f^4$ states are listed in Table X. The levels are listed in the first column. Next two columns of Table X lists possible transitions that give dominant contributions to the lifetimes given in the last column of Table X. The CI+all-order energies of lower and upper levels, taken from Table III, are given in the next two columns in cm^{-1}. The corresponding vacuum transition wavelengths λ are listed in the next column in Å. The values of the M1 matrix elements are given in Bohr magnetons. The transition rates A_r are calculated for the 79 M1 transitions, but only 42 transition rates that give significant contributions to the lifetimes are given. Lifetime values are given in milliseconds.

VII. CONCLUSIONS

In present paper, we evaluated the atomic properties of Cd-like W^{26+}, In-like W^{25+}, and Sn-like W^{24+} ions using the CI+all-order approach. The energies, transition rates, branching ratios, and lifetimes of the low-lying levels are evaluated.

We find an excellent agreement between the CI+all-order wavelengths and measurements for the Cd-like

TABLE X: Energies (in cm^{-1}), wavelengths (in Å), magnetic-dipole matrix elements (in μ_B), M1 transition rates (in s^{-1}), and lifetimes (in ms) in Sn-like W^{24+} ion evaluated using the CI+all-order method. The numbers in brackets represent powers of 10.

Level	Transition		Energies		λ	Z_{M1}	A_r	Br.ratio	τ, ms
$^5I_5^1$	$^5I_4$	$^5I_5^1$	0	13854	721.8	4.7134	1.45[2]	1.00	6.90
$^5I_6^1$	$^5I_5^1$	$^5I_6^1$	13854	25823	835.5	5.6691	1.15[2]	1.00	8.70
$^3D_1$	$^5F_2^1$	$^3D_1$	34776	39823	1981.4	2.3977	6.63[0]	1.00	150.
$^3G_4^1$	$^5I_4$	$^3G_4^1$	0	43458	230.1	1.1309	3.14[2]	0.83	2.66
	$^5I_5^1$	$^3G_4^1$	13854	43458	337.8	0.8966	6.26[1]	0.17	
$^5I_8$	$^5I_7$	$^5I_8$	35681	44030	1197.7	4.4020	1.79[1]	1.00	55.9
$^5F_3$	$^5F_2^1$	$^5F_3$	34776	46853	828.0	2.6802	4.87[1]	0.75	15.5
	$^5I_4$	$^5F_3$	0	46853	213.4	0.1952	1.51[1]	0.23	
$^3F_2^1$	$^5F_2^1$	$^3F_2^1$	34776	50423	639.1	1.1006	2.50[1]	0.97	38.7
$^3F_2$	$^3D_1$	$^3F_2$	39823	50458	940.3	1.6911	1.86[1]	0.37	19.8
	$^5F_2^1$	$^3F_2$	34776	50458	637.7	0.8756	1.59[1]	0.31	
	$^5F_2^1$	$^3F_2$	34777	50458	637.7	0.8775	1.60[1]	0.32	
$^5P_2$	$^5F_2^1$	$^5P_2$	34776	51659	592.3	1.2555	4.10[1]	0.97	23.8
$^1F_3^1$	$^5F_2^1$	$^1F_3^1$	34776	53468	535.0	1.9149	9.23[1]	0.62	6.76
	$^5I_4$	$^1F_3^1$	0	53468	187.0	0.2667	4.19[1]	0.28	
$^3K_6$	$^5I_5^1$	$^3K_6$	13854	56846	232.6	1.6090	4.27[2]	0.82	1.93
	$^5I_6^1$	$^3K_6$	25823	56846	322.3	1.2230	9.23[1]	0.18	
$^3G_5$	$^3G_4^1$	$^3G_5$	43458	59657	617.3	2.9256	8.92[1]	0.43	4.86
	$^5I_5^1$	$^3G_5$	13854	59657	218.3	0.5386	6.84[1]	0.33	
	$^5I_6^1$	$^3G_5$	25823	59657	295.6	0.6877	4.49[1]	0.22	
$^5L_7$	$^5I_7$	$^5L_7$	35681	60784	398.4	2.1715	1.34[2]	1.00	7.46
$^3F_4$	$^5I_4$	$^3F_4$	0	61321	163.1	0.3845	1.02[2]	0.31	3.05
	$^5F_3$	$^3F_4$	46853	61321	691.2	2.9845	8.09[1]	0.25	
	$^5I_5^1$	$^3F_4$	13854	61321	210.7	0.4564	6.68[1]	0.20	
	$^3G_4^1$	$^3F_4$	43458	61321	559.8	2.0518	7.19[1]	0.22	
$^1L_8$	$^5I_8$	$^1L_8$	44030	65662	462.3	3.1403	1.58[2]	0.61	3.87
	$^5I_7$	$^1L_8$	35681	65662	333.5	1.5261	9.94[1]	0.38	
$^3G_4^2$	$^5I_5^1$	$^3G_4^2$	13854	71981	172.0	0.5820	1.99[2]	0.29	1.45
	$^1F_3^1$	$^3G_4^2$	53468	71981	540.2	3.2498	2.01[2]	0.29	
	$^3G_4^1$	$^3G_4^2$	43458	71981	350.6	1.5075	1.58[2]	0.23	
	$^5I_4$	$^3G_4^2$	0	71981	138.9	0.3222	1.16[2]	0.17	
$^3D_2$	$^3D_3$	$^3D_2$	46853	73898	369.8	1.3265	1.88[2]	0.50	2.66
	$^5P_2$	$^3D_2$	51659	73898	449.7	1.4233	1.20[2]	0.32	
$^5G_5$	$^5I_6^1$	$^5G_5$	25823	74122	207.0	0.5796	9.27[1]	0.32	3.41
	$^5I_5^1$	$^5G_5$	13854	74122	165.9	0.3635	7.09[1]	0.24	
	$^3F_4$	$^5G_5$	61321	74122	781.2	3.4219	6.03[1]	0.21	
$^5G_3^1$	$^3F_2^1$	$^5G_3^1$	50423	74452	416.2	2.4301	3.16[2]	0.66	2.10
	$^5F_3$	$^5G_3^1$	46853	74452	362.3	1.2686	1.30[2]	0.27	
$^1P_1^1$	$^3D_1$	$^1P_1^1$	39823	80291	247.1	0.6120	2.23[2]	0.72	3.24
	$^3F_2$	$^1P_1^1$	50458	80291	335.2	0.5989	8.57[1]	0.28	

W^{26+} spectra [18], the differences are 0.02% - 0.04% for the $^1G_4 - ^3 F_4$, $^3F_3 - ^3 F_4$ and and $^3H_5 - ^3 H_6$ transitions and 0.2% - 0.4% for the $^1D_2 - ^3 P_2$, $^1G_4 - ^3 F_4$, $^3H_4 - ^3 H_5$, and $^3F_2 - ^3 F_3$ transitions. For In-like W^{25+} spectra, we observe excellent, 0.2% - 0.3%, agreement for wavelengths obtained by the CI+all-order method and experimental values from [10, 21]. This work provided the first extensive benchmark study of the CI+all-order method accuracy for the $4f^n$ states demonstrating excellent predictive properties of this approach for further use in new experiments and spectra identification.

Acknowledgments

This work is partly supported by the U.S. NSF Grant No. PHY-1620687.

[1] Y. Ralchenko, Plasma Fusion Res. **8**, 2503024 (2013).
[2] N. J. Peacock, M. G. O'Mullane, R. Barnsley, and M. Tarbutt, Can. J. Phys. **86**, 277 (2008).
[3] C. H. Skinner, Can. J. Phys. **86**, 285 (2008).
[4] J. C. Berengut, V. A. Dzuba, and V. V. Flambaum, Phys. Rev. Lett. **105**, 120801 (2010), arXiv:1007.1068.
[5] M. S. Safronova, ArXiv e-prints (2016), 1607.07932.
[6] A. Derevianko, V. A. Dzuba, and V. V. Flambaum, Phys. Rev. Lett. **109**, 180801 (2012).
[7] V. A. Dzuba, A. Derevianko, and V. V. Flambaum, Phys. Rev. A **86**, 054501 (2012).
[8] V. A. Dzuba, A. Derevianko, and V. V. Flambaum, Phys. Rev. A **87**, 029906 (2013).
[9] L. Schmöger, O. O. Versolato, M. Schwarz, M. Kohnen, A. Windberger, B. Piest, S. Feuchtenbeiner, J. Pedregosa-Gutierrez, T. Leopold, P. Micke, et al., Science **347**, 1233 (2015).
[10] W. Li, J. Xiao, Z. Shi, Z. Fei, R. Zhao, T. Brage, S. Huldt, R. Hutton, and Y. Zou, J. Phys. B **49**, 105002 (2016).
[11] V. Jonauskas, T. Pütterich, S. Kučas, Š. Masys, A. Kynienė, G. Gaigalas, R. Kisielius, L. Radžiūtė, P. Rynkun, and G. Merkelis, J. Quant. Spectrosc. Radiat. Transfer **160**, 22 (2015).
[12] A. Alkauskas, P. Rynkun, G. Gaigalas, A. Kynienė, R. Kisielius, S. Kučas, Š. Masys, G. Merkelis, and V. Jonauskas, J. Quant. Spectrosc. Radiat. Transfer **136**, 108 (2014).
[13] G. Gaigalas, P. Rynkun, A. Alkauskas, and Z. R. Rudzikas, At. Data Nucl. Data Tables **98**, 391 (2012).
[14] G. Gaigalas, Z. Rudzikas, P. Rynkun, and A. Alkauskas, Phys. Rev. A **83**, 032509 (2011).
[15] G. Gaigalas, Z. Rudzikas, E. Gaidamauskas, P. Rynkun, and A. Alkauskas, Phys. Rev. A **82**, 014502 (2010).
[16] X.-B. Ding, F. Koike, I. Murakami, D. Kato, H. A. Sakaue, C.-Z. Dong, N. Nakamura, A. Komatsu, and J. Sakoda, J. Phys. B **44**, 145004 (2011).
[17] V. Jonauskas, A. Kynienė, P. Rynkun, S. Kučas, G. Gaigalas, R. Kisielius, Š. Masys, G. Merkelis, and L. Radžiūtė, J. Phys. B **48**, 135003 (2015).
[18] Z. Fei, W. Li, J. Grumer, Z. Shi, R. Zhao, T. Brage, S. Huldt, K. Yao, R. Hutton, and Y. Zou, Phys. Rev. A **90**, 052517 (2014).
[19] L. Glowacki and J. Migdalek, J. Phys. B **36**, 3629 (2003).
[20] H. A. Sakaue, D. Kato, N. Yamamoto, N. Nakamura, and I. Murakami, Phys. Rev. A **92**, 012504 (2015).
[21] A. Komatsu, J. Sakoda, M. Minoshima, H. A. Sakaue, X. B. Ding, D. Kato, I. Murakami, F. Koike, and N. Nakamura, Plasma and Fusion Research **7**, 1201158 (2012).
[22] M. S. Safronova, M. G. Kozlov, W. R. Johnson, and Dansha Jiang, Phys. Rev. A **80**, 012516 (2009).
[23] M. S. Safronova, W. R. Johnson, and A. Derevianko, Phys. Rev. A **60**, 4476 (1999).
[24] M. S. Safronova and U. I. Safronova, Phys. Rev. A **83**, 012503 (2011).
[25] M. S. Safronova, V. A. Dzuba, V. V. Flambaum, U. I. Safronova, S. G. Porsev, and M. G. Kozlov, Phys. Rev. A **90**, 042513 (2014).
[26] M. S. Safronova, V. A. Dzuba, V. V. Flambaum, U. I. Safronova, S. G. Porsev, and M. G. Kozlov, Phys. Rev. A **90**, 052509 (2014).
[27] M. S. Safronova, V. A. Dzuba, V. V. Flambaum, U. I. Safronova, S. G. Porsev, and M. G. Kozlov, Phys. Rev. Lett. **113**, 300801 (2014).
[28] M. S. Safronova and W. R. Johnson, Adv. At. Mol., Opt. Phys. **55**, 191 (2007).
[29] M. S. Safronova, M. G. Kozlov, and U. I. Safronova, Phys. Rev. A **85**, 012507 (2012).
[30] Z. Zuhrianda, M. S. Safronova, and M. G. Kozlov, Phys. Rev. A **85**, 022513 (2012).
[31] M. S. Safronova, S. G. Porsev, M. G. Kozlov, and Charles W. Clark, Phys. Rev. A **85**, 052506 (2012).
[32] S. G. Porsev, M. S. Safronova, and M. G. Kozlov, Phys. Rev. Lett. **108**, 173001 (2012).
[33] M. S. Safronova, U. I. Safronova, and S. G. Porsev, Phys. Rev. A **87**, 032513 (2013).
[34] M. S. Safronova and P. K. Majumder, Phys. Rev. A **87**, 042502 (2013).
[35] M. S. Safronova, V. A. Dzuba, V. V. Flambaum, U. I. Safronova, S. G. Porsev, and M. G. Kozlov, Phys. Rev. Lett. **113**, 030801 (2014).
[36] I. Savukov, U. I. Safronova, and M. S. Safronova, Phys. Rev. A **92**, 052516 (2015).
[37] V. A. Dzuba, M. S. Safronova, and U. I. Safronova, Phys. Rev. A **90**, 012504 (2014).
[38] V. A. Dzuba, M. S. Safronova, U. I. Safronova, and A. Kramida, Phys. Rev. A **94**, 042503 (2016).
[39] M. S. Safronova, U. I. Safronova, and Charles W. Clark, Phys. Rev. A **91**, 022504 (2015).
[40] M. G. Kozlov, S. G. Porsev, M. S. Safronova, and I. I. Tupitsyn, Comp. Phys. Comm. **195**, 199 (2015).
[41] A. Bar-Shalom, M. Klapisch, and J. Oreg, J. Quant. Spectrosc. Radiat. Transfer **71**, 169 (2001).
[42] P. Jö?nsson, X. He, C. F. Fischer, and I. Grant, Comput. Phys. Commun. **177**, 597 (2007).
[43] S. Fritzsche, J. Electron Spectrosc. Relat. Phenom. **114-116**, 1155 (2001).
[44] M. F. Gu, Can. J. Phys **86**, 675 (2008).